



The colorful giants: Revisiting the systematics of the *Anolis latifrons* series (Squamata: Anolidae)

Carlos M. Marín¹, Daniel Bocanumenth², Juan M. Daza²

¹ Laboratorio de Macroecología Evolutiva, Red de Biología Evolutiva, Instituto de Ecología A.C., Veracruz, CP, 91073, Mexico

² Grupo Herpetológico de Antioquia GHA, Instituto de Biología, Facultad de Ciencias Exactas y Naturales, Universidad de Antioquia UdeA, Calle 70 No. 52-21, Medellín, Colombia

<https://zoobank.org/8134FAA0-D9C8-4682-94BE-644982083A9F>

Corresponding author: Juan M. Daza (jumadaza@gmail.com)

Academic editor Uwe Fritz | Received 17 June 2025 | Accepted 28 September 2025 | Published 29 October 2025

Citation: Marín CM, Bocanumenth D, Daza JM (2025) The colorful giants: Revisiting the systematics of the *Anolis latifrons* series (Squamata: Anolidae). *Vertebrate Zoology* 75: 441–457. <https://doi.org/10.3897/vz.75.e162071>

Abstract

The lizard genus *Anolis* is the second most diverse genus of terrestrial vertebrates. Within *Anolis*, the highly speciose clade *Dactyloa* comprises six species series, including the *latifrons* series. Despite previous efforts to reconstruct its phylogeny, earlier studies have excluded a substantial proportion of the clade's species diversity. Here, we integrated both historical and newly generated genetic data to reconstruct the most comprehensive molecular phylogeny of the *latifrons* series to date including 88% of the current species diversity. We also conducted a thorough morphological examination of museum specimens representing ten species, primarily distributed in Colombia, including vouchers of *A. danieli* from the Central Cordillera used in previous molecular phylogenies. Our phylogeny also included genetic samples of *A. danieli* from several localities in the Western Cordillera, samples of *Anolis limon* and *A. mirus* (two species previously lacking genetic data), and sequences from the Central American species *A. kathydayae* and *A. brooksi*. Our results recovered topological differences for *A. limon* and *A. mirus* compared to previous hypotheses and revealed that specimens assigned to *A. danieli* in earlier studies were misidentified and are not phylogenetically related to this species. Instead, our results showed that the true *A. danieli* is sister to a green anole clade distributed across the Central Cordillera, Pacific region, and Panama. Based on our phylogenetic and genetic distance analyses, we conclude that *A. kathydayae* should be considered a junior synonym of *A. brooksi*. Lastly, we describe the taxon previously confused with *A. danieli* and comment on the taxonomic implications of our findings.

Keywords

Biogeography, *Dactyloa*, morphometrics, Neotropics, species description, systematics

Introduction

The Neotropical lizard genus *Anolis* Daudin, 1802, with 434 species (Uetz et al. 2025), is recognized as the second most diverse genus of terrestrial vertebrates after the rainfrog genus *Pristimantis* Jiménez De La Espada, 1870 (Poe et al. 2017; Christodoulides et al. 2024). The outstanding species richness, high levels of cryptic diversity (Yáñez-Muñoz et al. 2018; Moreno-Arias et al. 2023) and

incomplete geographic and genetic sampling in mainland regions across South America, including the Andes and the Amazonia, have hampered accurate species delimitation within several groups (Velasco and Hurtado-Gómez 2014; Grisales-Martínez et al. 2017; Prates et al. 2020). As a result, a substantial proportion of the genus diversity is still to be discovered. Within *Anolis*, the clade *Dac-*

tyloa Wagler, 1830 comprises large-bodied species primarily found on the South American mainland, as well as a smaller, less diverse radiation in the Lesser Antilles (Castañeda and de Queiroz 2011, 2013). Currently, six species groups (Williams 1976) or series (Savage and Guyer 1989) are recognized within *Dactyloa*, including the *punctatus*, *roquet*, *heterodermus*, *aequatorialis*, and *latifrons* series and the more recently proposed *nasofrontalis* series by Prates et al. (2020).

The *latifrons* series was first proposed by Etheridge (1960) to accommodate three species: *Anolis latifrons* Berthold, 1846, *A. frenatus* Cope, 1899 and *A. fraseri* Günther, 1859. The taxonomic content of this series, as originally circumscribed, remained largely unchanged until molecular and morphological data began to be generated by studies that tested its monophyly (Poe 2004; Velasco and Hoyos 2010; Castañeda and de Queiroz 2011, 2013). The species content of the series has varied significantly as recent studies have added new species to the group (Poe et al. 2015; Poe and Ryan 2017; Prates et al. 2020). Currently, the *latifrons* series includes 25 named species distributed across the lowlands of Panama, Costa Rica, Venezuela, Ecuador, the Pacific region (including Malpelo island), and the inter-Andean valleys of Colombia (Castañeda and de Queiroz 2011, 2013; Poe et al. 2017; Prates et al. 2020).

The most comprehensive phylogeny of the *latifrons* series to date, published by Poe et al. (2017), assessed evolutionary relationships by incorporating morphological data for species lacking DNA sequences into a primarily molecular framework. This approach raises concerns about the reliability of phylogenetic placements for taxa without genetic data, particularly when evaluated from a strictly molecular standpoint. More importantly, the phylogeny of Poe et al. (2017), along with subsequent studies based exclusively on molecular data (e.g., Batista et al. 2015; Prates et al. 2017, 2020; Ayala-Varela et al. 2021), failed to include a substantial portion of the group's species diversity. For example, Poe et al. (2017) included 20 of the 24 species recognized at the time; however, DNA sequences were unavailable for 25% of the evaluated taxa. More recent molecular phylogenies have included between 52% and 80% of the species (Prates et al. 2017; Ayala-Varela et al. 2021). Remarkably, the more recent studies omitted *A. brooksi* (Barbour, 1923) despite the availability of molecular data for this taxon. This situation underscores the need for an updated phylogeny that incorporates most of the currently recognized diversity in the series and evaluates the placement of species previously excluded from molecular phylogenies due to missing sequence data.

Despite efforts to reconstruct the phylogeny of the *latifrons* series (e.g., Velasco and Hoyos 2010; Castañeda and Queiroz 2011, 2013; Prates et al. 2017, 2020) several gaps remain concerning the taxonomic identity, phylogenetic position, and geographical distribution of several species. One such example is *Anolis danieli* Williams, 1988, originally described from the municipality of Uriarao in Antioquia, Colombia. In addition to the type lo-

cality, this species is known from several other localities in the northwestern Cordillera in Colombia (Velasco and Hoyos 2010). Nonetheless, despite its well-known distribution, the only genetic samples labeled as *Anolis danieli*, included for the first time in the phylogenetic analyses by Castañeda and de Queiroz (2011) and then in a series of subsequent studies (see Castañeda and de Queiroz 2013; Poe et al. 2017; Prates et al. 2020), were collected at the northern region of the Central Cordillera in the municipality of Anori. Therefore, neither samples from the species' type locality nor its surroundings in the Western Cordillera have been included in molecular phylogenetic analyses so far, and consequently, the phylogenetic affinities between western and central populations remain entirely unknown.

Velasco and Hoyos (2010) noted that the morphological traits of individuals assigned to *Anolis danieli* from the municipality of Anori, Antioquia do not match the diagnostic characters of the species' type series. We confirm this observation through our own examination of specimens from Anori, including the voucher specimens used in the phylogeny of Castañeda and de Queiroz (2011), as well as a reexamination of the type series of *A. danieli*. These observations indicate that the sample analyzed by Castañeda and de Queiroz (2011) were misidentified as *A. danieli*. Therefore, the phylogenetic position of this species within the *latifrons* series remains poorly understood. Additionally, the phylogenetic position of other species, including *A. limon* Velasco & Hurtado-Gómez, 2014 and *A. mirus* Williams, 1963, have been assessed solely based on morphological data, leaving their placement in molecular phylogenies uncertain.

In this study, we combined both published and newly generated molecular data to reconstruct the phylogeny of the *latifrons* series and test the phylogenetic positions of two species for which previous phylogenies incorporated only morphological information. We also gathered morphological and geographical data to formally describe the taxon previously assumed to be *A. danieli*. We expect this study to clarify the phylogenetic relationships, morphological variation, and geographic distribution of species in the *latifrons* series, thereby contributing to a broader understanding of the biodiversity patterns within the highly diverse *Dactyloa* clade.

Methods

Institutional acronyms

We examined the available material of the *latifrons* series housed in the following Colombian herpetological collections: Museo de Herpetología Universidad de Antioquia (MHUA), Colecciones Biológicas Universidad CES (CBUCES), Museo de Ciencias Naturales de La Salle (CSJ), and Colección Biológica Universidad EAFIT (EAFIT).

Taxon sampling

We examined specimens of *Anolis apollinaris* Boulenger, 1919, *A. danieli* (including the holotype), *A. fraseri*, *A. frenatus*, *A. latifrons*, *A. limon* (including the holotype), *A. maculigula* Williams, 1984, *A. princeps* Boulenger, 1902, *A. purpurescens* Cope, 1899, an undescribed species previously allocated to the *latifrons* series (i.e., *A. sp.2* from Castañeda and de Queiroz 2011) and specimens identified to the genus level (i.e., *Anolis sp.*). In addition, we included the only known (to our knowledge) specimens of *A. mirus* beyond its type locality in the western region of Colombia. In total we gathered morphometric and meristic data for 200 specimens. From these specimens we generated genetic data for the following species (number of sequenced specimens in parentheses): *A. maculigula* (2), *A. latifrons* (4), *A. frenatus* (3), the lineage labeled as *A. danieli* by Castañeda and de Queiroz (2011) (8), the true *A. danieli* (12), *A. purpurescens* (1) and, for the first time within the Dactyloa clade, we generated sequences for both *A. limon* (2) and *A. mirus* (1).

DNA sequence data and phylogenetic analyses

We amplified and sequenced: a partial region of the mitochondrial ribosomal unit 16S using the primers 16SCL-16SDH (Santos et al. 2009) and 16Sar-16Sbr (Santos et al. 2003), a partial region of the cytochrome oxidase subunit 1 COI using the primers repCOI-F-repCOI-R (Palumbi 1996), and a partial region of the NAD dehydrogenase subunit 2 ND2 using the primers metf6-L5556 (Castañeda and de Queiroz 2011). We combined these newly generated sequences with available sequences for these three regions and the nuclear regions ECEL1 and rag1 from GenBank (www.ncbi.nlm.nih.gov/Genbank) and the Steven Poe's webpage (<https://www.stevenpoe.net>). In total for the *latifrons* series, we obtained 199 sequences (65 generated by us and 134 gathered from previous studies), representing 22 out of the 25 named species of the group (88% of the its known richness). For the remaining species, namely *Anolis propinquus* Williams, 1984, *A. squamulatus* Peters, 1863 and *A. savagei* Poe & Ryan, 2017, no genetic data are available; therefore, they were not included in our assembled dataset.

We aligned each region using MAFFT under default parameters (Kato and Standley 2013). We assembled a single matrix and used ModelFinder (Kalyaanamoorthy et al. 2017) to determine the best partition scheme and the evolutionary model for each partition. We inferred a phylogenetic tree using Maximum Likelihood as implemented in IQTREE 2 (Minh et al. 2020). Nodal support was estimated with 5000 pseudoreplicates using the ultrafast bootstrap approach (Minh et al. 2013). We then estimated raw genetic distances using the 16S fragment (the region with more sequences available) using the *dist.dna* function in the *ape* R package (Paradis et al. 2004).

Morphological data

We assembled a dataset with 24 morphometric variables: 16 linear and eight meristic. Linear measurements and meristic traits were selected following Köhler (2014) and Williams et al. (1995) respectively. In total, we obtained morphometric data from 200 specimens corresponding to ten formally described species and two undescribed taxa according to Castañeda and de Queiroz (2011), namely, *Anolis sp.1* and *A. sp.2*. Our dataset also includes 42 samples of *Anolis danieli* from across its geographic distribution (33 samples from the Western Cordillera and 9 from the Central Cordillera). Linear variables are: **HL** (head length), **HW** (head width), **HH** (Head height), **SL** (snout length), **LDE** (length of the meatus), **LDP** (length of the interparietal scale), **HuL** (humerus length), **UIL** (ulnae length), **FL** (femur length), **FoL** (foot length), **ShL** (shank length), **H** (hand length), **Fourth_L** (fourth toe length), **SPW** (subdigital pad width), **TL** (tail length) and **SVL** (snout-vent length). We measured **H** and **FL** since these variables were used by Ayala-Varela (2021) to compare *A. nemontae* with its related species *A. fraseri*. Meristic variables are: **Canths_2** (number of scales between second canthals), **PR** (number of postrostral scales), **IO** (number of scales between supraorbital semicircles), **IP/IO** (number of scales between interparietal and semicircles), **SPLeve** (number of supralabial scales to the level below center of the eye), **PM** (number of postmental scales), **ToeLam2_3** (Counting the plates under phalanges II–III) and **ToeLam2_4** (Counting the plates under phalanges II–IV). We counted this latter character following both Williams et al. (1995) and Köhler (2014) to facilitate species comparisons, as the nomenclature of this trait varies across studies. Linear measurements were taken under the stereo microscope with a digital caliper to the nearest 0.1 mm. Measurements of museum vouchers examined in this study and associated geographic data are available in the File S1. Sex was determined by the presence of hemipenis and, in some species, by the presence of enlarged postcloacal scales in males. Dewlap size was also used as a sexually dimorphic character: in males, the dewlap extends posteriorly beyond the level of the forelimb insertion, whereas in females it does not. The coloration description was based on field observations and photos of live specimens. Comparisons with congeneric species of the *latifrons* series were conducted by a detailed examination of original descriptions and specimens housed in the herpetological collections visited (see the Taxon sampling section).

Morphometric analyses

To evaluate the morphologic distinctiveness among species of the *latifrons* series, we conducted a discriminant analysis coupled to a principal component analysis (**DAPC**; Jombart et al. 2010) on our assembled measurements and meristic dataset. DAPC is a supervised method that utilizes a linear combination of intercorrelated

descriptors to maximize between-group variance while minimizing within-group variance, allowing individuals from predefined species to be assigned to distinct clusters. Implementation of DAPC is preferable over other multivariate approaches such as PCA alone, which focuses on trait covariation but ignores the cluster identity of individuals, potentially overlooking actual differences among groups (Jombart et al. 2010). Nineteen individuals lacked linear measurements for TL due to incomplete tails. Thus, to include these specimens in our morphometric analysis, we employed a missing data imputation approach. Specifically, we used the mean value for this continuous trait calculated across all individuals of a given species and considering only adult specimens. We conducted the DAPC analysis using species identity as the output variable and morphometric values as the input variables.

To estimate the minimum number of principal components accounting for the highest morphological covariation and predicted cluster membership, we used cross-validation with 90% of the data for training, 10% for testing, and 300 replicates at each level of PCA retention. Cross-validation analysis aims at selecting the number of principal components (PCs) that maximize the mean success assignment while minimizing the root square error of assignments (e.g., <1% of successful rate assignment) or the lower number of PCs. The optimal number of PCs was selected through cross-validation, and we retained the lowest number of discriminant functions that allowed classification success rates above 90%.

To determine which type of dataset, based on either linear measurements or meristic data, most effectively distinguishes among the examined species, we performed DAPC analyses on three independent datasets: 1 – only linear measurements (LM), 2 – only meristic data (MD), and 3 – a combined dataset (CD) containing both linear measurements and meristic data. Our morphometric analyses included only adult specimens from species with measurements available for more than two individuals. Cross-validation and DAPC analyses were conducted using the adegenet R package (Jombart 2008; R Core Team 2025).

Results

Phylogenetic inference

The assembled matrix included 235 terminals and 5533 segregating sites. The best partition scheme and substitution models were: GTR+F+I+R4 (16S), SYM+I+G4 (COI_1), F81+F+I+R2 (COI_2), TIM2+F+R7 (COI_3+ND2_3), TR+F+I+R5 (ND2_1), TVM+F+I+R5 (ND2_2), and TIM3+F+R2 (ECEL1+RAG1). The obtained phylogenetic tree was well supported with most of the nodes with UFB>95% (Fig. 1). Although our phylogenetic tree represents the most comprehensive analysis of the *latifrons* series to date, many of the relationships we recov-

ered are consistent with the hypothesis proposed by Poe et al. (2017), which integrated both morphological and genetic data (Fig. 2). Minor topological differences with respect to previous studies involve species for which we generated novel sequences, and these are highlighted as follows: *Anolis limon* was recovered as the sister species to the clade comprising *A. purpurescens*, *A. ibanezi* Poe, Latella, Ryan & Schaad, 2009, and *A. maia* (Batista et al., 2015), rather than as the sister to the clade comprising *A. purpurescens* and *A. ibanezi*, as reported by Poe et al. (2017). Our results also differ from those of Batista et al. (2015), who recovered *A. maia* as sister to the clade comprising *A. ibanezi* and *A. purpurescens*, whereas our analysis supports *A. maia* as the sister species to *A. ibanezi*. Likewise, our tree recovers *A. mirus* as the sister taxon to the clade comprising *A. parilis* Williams, 1975, *A. fraseri*, and *A. nemontae* Ayala-Varela et al., 2021, in contrast to Poe et al. (2017), who recovered *A. mirus* as the sister species of *A. kunayalae* Hulebak, Poe, Ibáñez & Williams, 2007 (Figs 1, 2). A full tree including 235 anole species and the corresponding matrix alignment and partitions scheme are available in Files S2–S4 respectively. ENA/GenBank accession numbers for species of the *latifrons* series used in this study including novel generated sequences are available in the File S1.

Our most significant finding, which contrasts with previous hypotheses, concerns the phylogenetic position of *Anolis danieli*. Castañeda and de Queiroz (2011) included genetic samples identified as *A. danieli*. However, upon examining those specimens, reviewing the holotype and paratype, and incorporating additional specimens and genetic data, we determined that the samples used in previous studies represent an undescribed taxon. We also included genetic data from specimens we consider to be the true *A. danieli*, collected from multiple localities, including sites near the type locality. Our analyses recovered *A. danieli* as sister, with 100% UFB support, to a clade comprising *A. purpurescens*, *A. maia*, *A. ibanezi*, and *A. limon* (Figs 1, 2). The new taxon, previously misidentified as *A. danieli*, was found to be sister to another undescribed species from the Santander department (Fig. 1). The genetic sample labeled as *A. sp.1* by Castañeda and de Queiroz (2011) was found to be nested within the clade representing the true *A. danieli*. In addition, our molecular phylogeny included *A. brooksi* and the recently described species *Anolis kathydayae* Poe & Ryan, 2017 but found them to show no evidence of genetic differentiation (Figs 1–3).

Overall, the interspecific genetic distances in the *latifrons* series ranged from 2% to 9% (Fig. 3). However, a particular case involves the genetic distances among *A. insignis* Cope, 1871, *A. kathydayae*, and *A. brooksi*. In the inferred phylogeny, *A. insignis* is clearly separated from the clade comprising (*A. kathydayae* + *A. brooksi*). Although there is an imbalance in genetic marker representation for these terminals (File S3), analysis of the COI region shows an uncorrected genetic distance of 10% between *A. insignis* (POE2015) and *A. brooksi* (File S5). In contrast, analysis of the 16S region reveals an uncorrected genetic distance of 0% between the

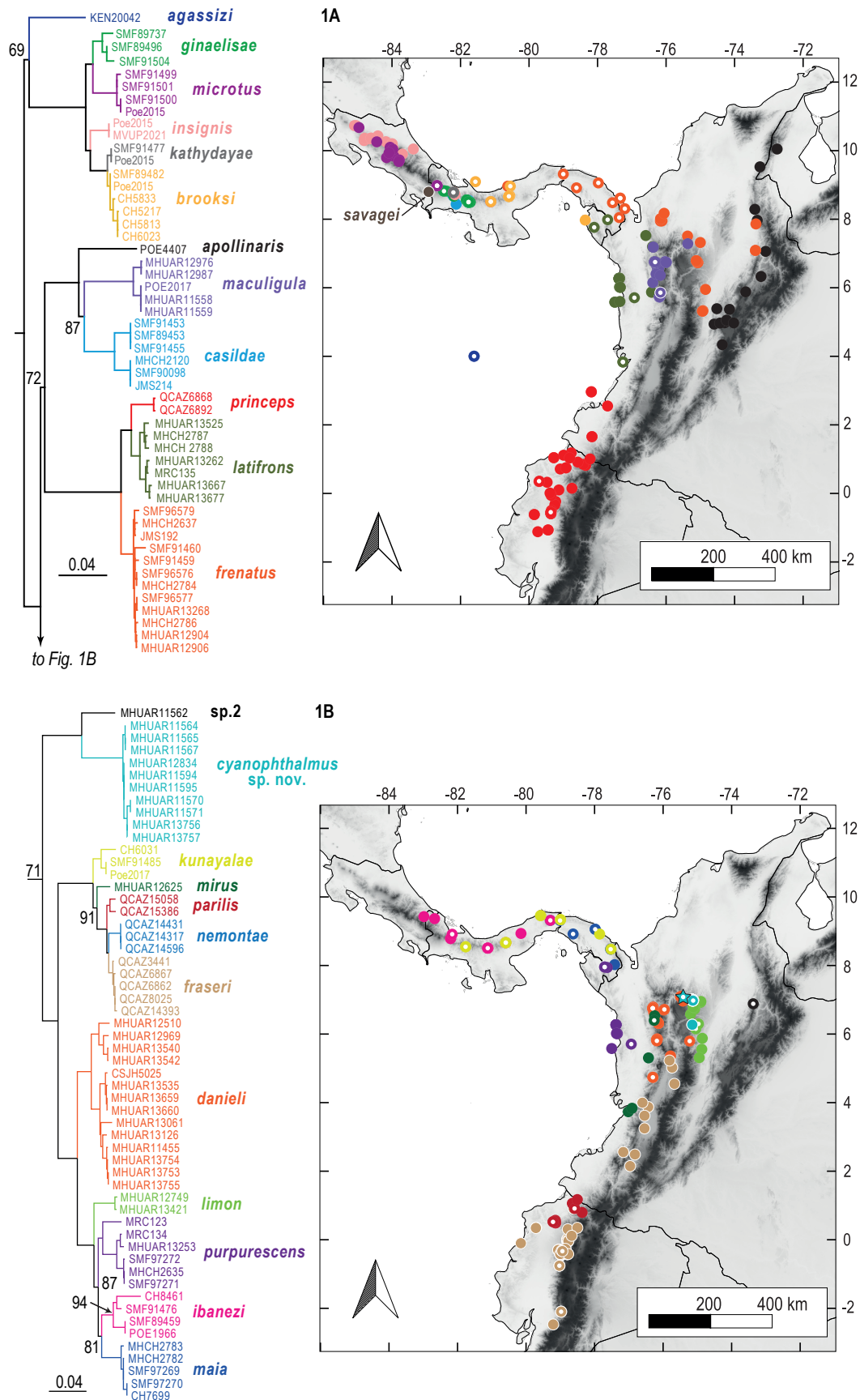


Figure 1. A, B Phylogenetic relationships among species of the *latifrons* series as inferred from molecular data. The geographic distribution of each lineage is depicted, with the colors of the tree tips corresponding to the dots on the map. Geographic occurrences for species not included in our main morphological dataset were taken from Velasco et al. (2020). Dots colored with white marks in the center represent sequenced voucher included in the phylogeny. Locality record for *A. savagei* is indicated on the map but this species was not included in the phylogeny since no molecular data are available. Star symbol represents the type locality of *Anolis cyanophthalmus* sp. nov.

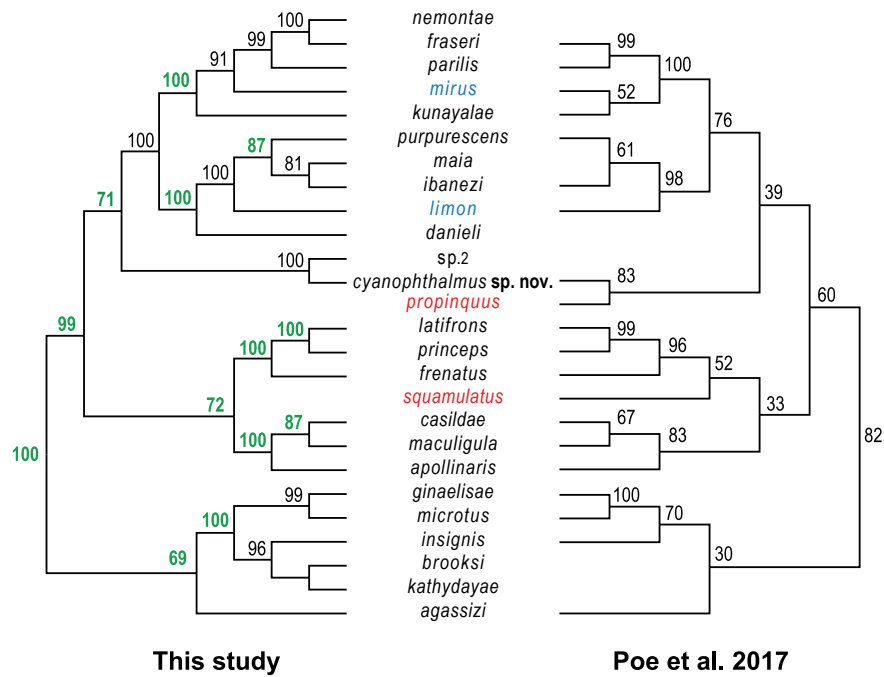


Figure 2. Comparison of our molecular phylogeny with the comprehensive phylogeny of the *latifrons* series by Poe et al. (2017). Blue tips indicate lineages for which we added genetic sequences for the first time. Red tips represent those species for which no molecular data are available. Green numbers indicate nodes present in Poe et al. (2017) but with lower support values.

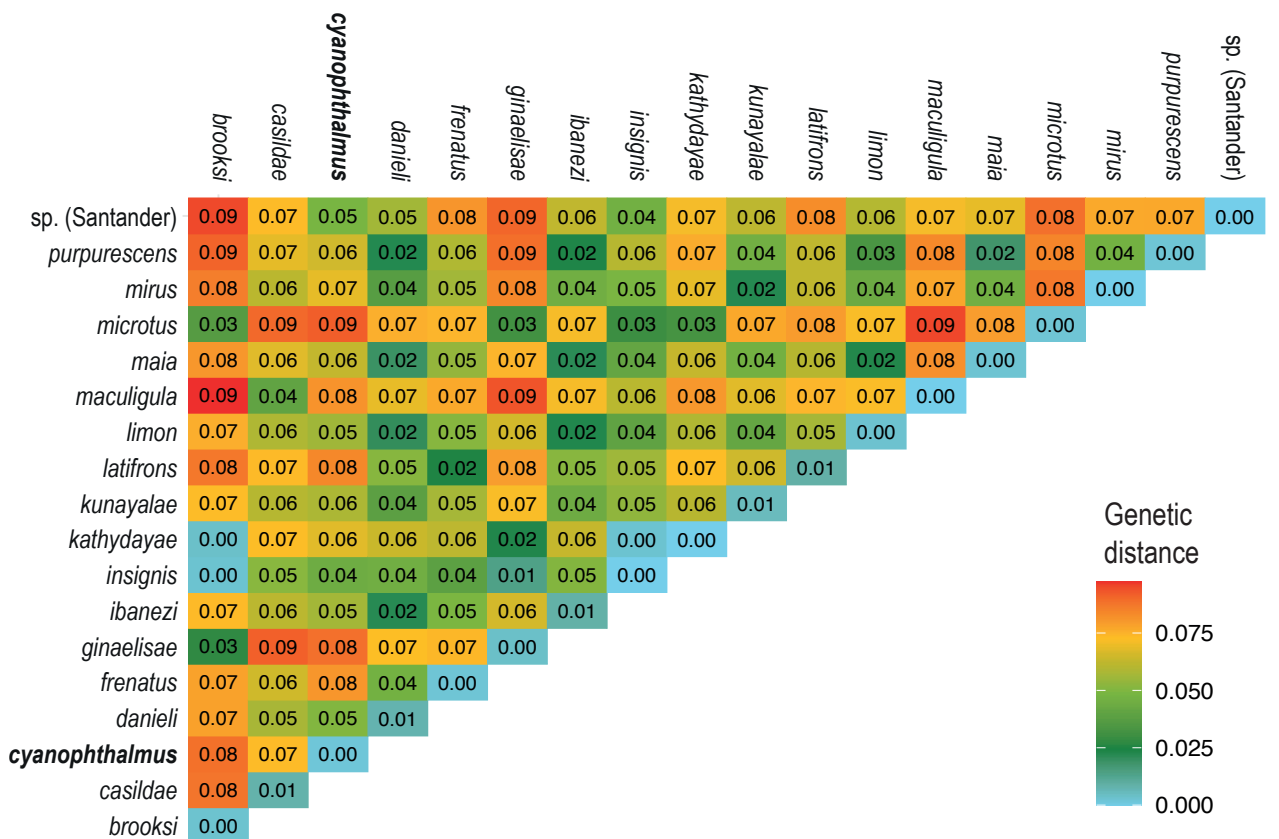


Figure 3. Heat map of estimates of net uncorrected genetic distances between species of the *latifrons* series as estimated using sequences of the 16S fragment. Note the lack of genetic divergence (light blue) between samples of *A. brooksi* and *A. kathydayae*.

same species (Fig. 3). While it is well established that COI evolves faster than 16S, such an extreme discrepancy between the two markers is unexpected. Notably, *A. insignis* (tip labeled POE2015 in Fig. 1) is not asso-

ciated with a voucher specimen, and its sequence is not available in GenBank; we retrieved it instead from the supplementary material of Poe et al. (2017). Therefore, the interspecific relationships shown in our phylogeny

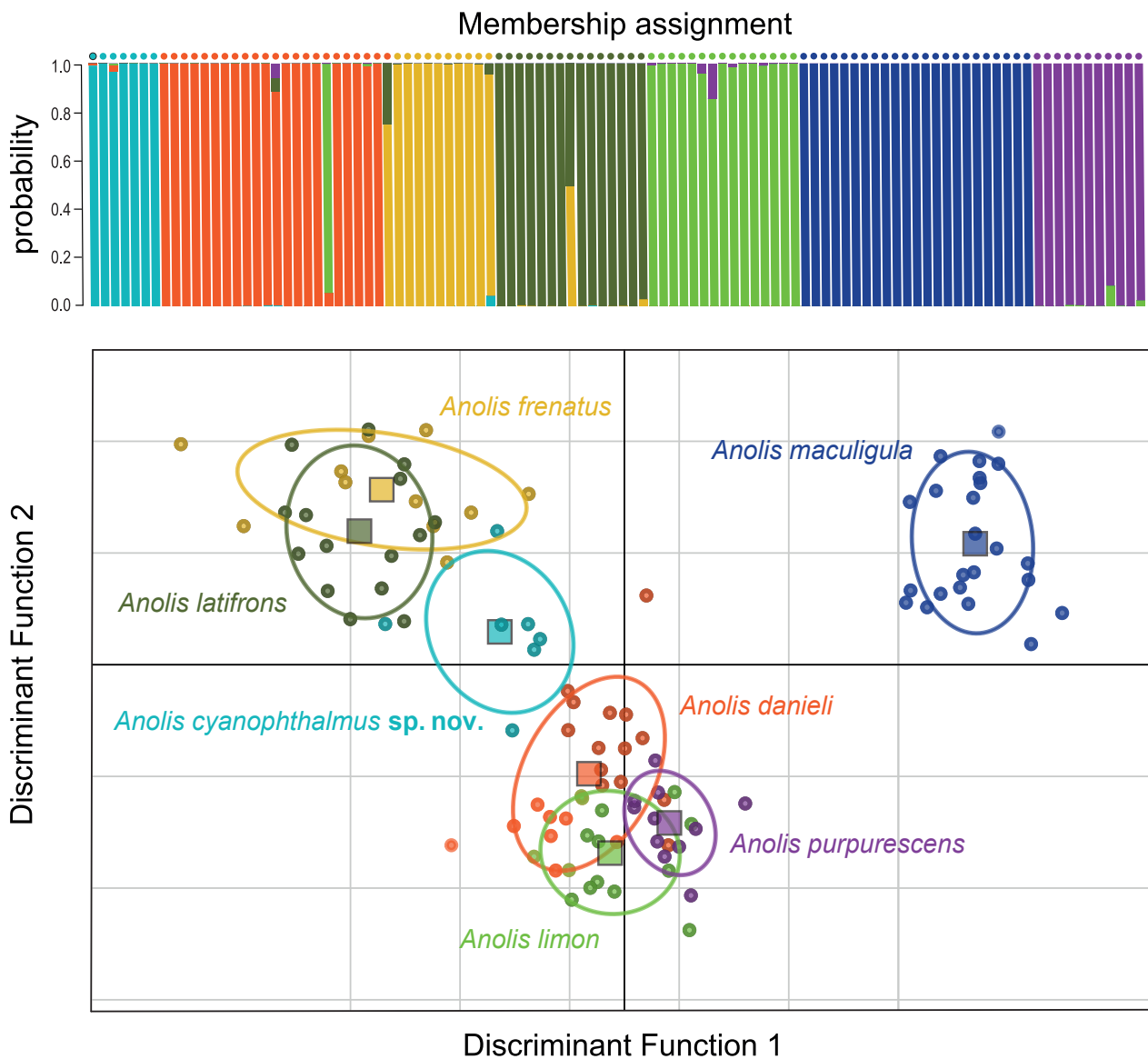


Figure 4. Morphometric differences among species of the *latifrons* series inferred from a DAPC analysis using the LM dataset. The top panel shows the posterior probability of individual assignment to each species (bars), relative to their actual species identity (filled circles). The bottom panel displays individuals in the morphometric space as represented by the first two discriminant functions. Inertia ellipses are included to facilitate visualization of group clustering.

for this small subclade were mainly resolved by the COI region.

Morphological analysis

After filtering for adults only, the final dataset used for the morphometric analyses included 109 individuals. The DAPC analysis successfully assigned between 91% (MD and CD datasets) and 99% (LM dataset) of these individuals to the appropriate species, including samples of the true *Anolis danieli* and the new taxon (Fig. 4) by summarizing the original morphometric variables into 13 PCs in the LM dataset, 6 PCs in the MD dataset, and 16 PCs in the CD dataset. These principal components were then combined into 6 discriminant functions (DFs) in both the LM and MD datasets, and eight DFs in the CD dataset. Most misclassification (nine) occurred in the analysis of

the MD dataset, where several species showed substantial overlap. In contrast, using both the LM and CD datasets resulted in the misclassification of only one individual.

Results from the LM dataset revealed morphometric differences among species primarily related to the variables LDE (0.58), HH (0.13), and LDP (0.10). Most differences in both the MD and CD datasets were associated with the variable IP/IO (0.43 and 0.33, respectively). In the LM dataset, the second discriminant function showed the strongest correlations with the variable HL (0.31), while in the MD and CD datasets, it was strongly correlated with the variables ToeLam2_3 and PR (0.39 and 0.15 respectively), as well as with PM (0.34 and 0.12 respectively). All this morphometric variation was independent of body size (SVL), which contributed less than 0.6% to each discriminant function. Since both the LM and CD datasets were quantitatively similar, we present our results based on the LM dataset (Fig. 4).

Discussion

In this study, we integrated historical and newly generated genetic data, including the first available sequences for two species in the *latifrons* series to reconstruct the most comprehensive molecular phylogeny of the clade to date. Based on our phylogenetic results, we tested the placement of these species and evaluated the species boundaries of two recently described Central American taxa. Through a thorough morphological examination of museum specimens, we determined that the taxon labeled as *Anolis danieli* in previous phylogenies was misidentified and actually corresponds to an undescribed species. In addition, we expanded the geographic and genetic sampling for the true *A. danieli* within the phylogeny of the *latifrons* series. Below, we discuss our main findings in detail.

Phylogenetic position of *Anolis danieli*, *A. limon* and *A. mirus*

Phylogenetic studies that have addressed the evolutionary relationships within the *latifrons* series have included either morphological or molecular samples of the nominal species *Anolis danieli* (Velasco and Hoyos 2010; Castañeda and de Queiroz 2011, 2013). In this study, we conducted a phylogenetic analysis of the *latifrons* series, including genetic samples of *A. danieli* from across its known geographic range in the Western Cordillera, and analyzed these samples along with those from the municipality of Anorí and other localities in the northern Antioquia, including samples used in all previous molecular phylogenies of the *latifrons* series. Strikingly, our analyses showed that samples assigned to *A. danieli* by Castañeda and de Queiroz (2011) do not actually correspond to this species. Instead, they represent an undescribed taxon, which had been consistently misidentified in prior phylogenetic studies (Castañeda and de Queiroz 2011, 2013; Prates et al. 2017; Prates et al. 2020). The phylogenetic position of the new taxon, as sister to an undescribed species from the Eastern Cordillera in the department of Santander (*A. sp.2* sensu Castañeda and de Queiroz 2011), is consistent with prior hypotheses (Castañeda and de Queiroz 2011, 2013; Prates et al. 2017, 2020). However, unlike earlier studies, our analyses retrieved *A. danieli* (i.e., *A. sp.1*, sensu Castañeda and de Queiroz 2011) as sister to the remaining green anoles from the midlands of the Central Cordillera and the lowlands of the Pacific region and Panama (Fig. 1).

Our results also help clarify the phylogenetic positions of two species that had previously been placed in the phylogeny of the group based solely on morphology due to the absence of molecular data. The first species, *Anolis limon*, was initially proposed by Velasco and Hurtado-Gómez (2014) as the sister species to *A. ibanezi*. Later, Poe et al. (2017), in their systematic assessment of the entire genus *Anolis*, recovered *A. limon* as the sister

species to the clade comprising *A. ibanezi* and *A. chocorum* (*A. purpurescens*). Contrary to these previous hypotheses, our phylogeny recovered *A. limon* as sister to the clade comprising *A. purpurescens*, *A. ibanezi*, and *A. maia*. The second species, *Anolis mirus*, was suggested to be part of the *aequatorialis* series by Williams (1975), Ayala-Varela and Velasco (2010), and Castañeda and de Queiroz (2013) although none of these studies conducted a formal test of its phylogenetic position. Poe et al. (2017) later placed *A. mirus* within the *latifrons* series as sister to *A. kunayalae*. However, contrary to these earlier hypotheses, our analysis recovered *A. mirus* as the sister species to the clade comprising *A. parilis*, *A. nemontae*, and *A. fraseri*.

Evaluating the utility of morphological data for the taxonomy of the *latifrons* series

The LM dataset performed the best in distinguishing among species of the *latifrons* series. Overall, the cluster formed by *A. danieli*, *A. limon*, and *A. purpurescens* showed significant overlap in the morphometric space. Although we were unable to include data for *A. ibanezi*, its morphological similarity to the remaining species of the clade in which it is nested suggests that the observed overlap pattern would likely persist with its inclusion in morphometric analysis. *Anolis frenatus* and *A. latifrons* also showed substantial morphometric overlap, likely reflecting their similarity in body size and limb proportions. Likewise, although we did not include samples from *A. princeps*, we suspect this species would also exhibit a high degree of morphometric overlap with the cluster comprising *A. frenatus* and *A. latifrons*, likely reflecting their conserved external morphology and phylogenetic proximity. Indeed, this similarity has led previous authors to question the validity of these taxa as distinct species (Savage and Talbot 1978; Williams 1988).

In contrast, the MD dataset did not allow for a clear distinction among the species of the *latifrons* series, with the notable exception of *Anolis maculigula*, which strongly segregates in the morphometric space across all datasets. This is likely due to *A. maculigula* possessing the highest number of scales between the second canthals among the species examined (Table 1). Based on these findings, we recommend future morphometric studies of the *latifrons* series to prioritize the analysis of linear measurements, as meristic traits alone seem to offer limited resolution for distinguishing among species in this group. Recent morphometric assessments of the Andean (Grisales-Martínez et al. 2017) and Central American fuscoauratoids (Köhler and Sunyer 2008; Ponce and Köhler 2008) have reached similar conclusions, suggesting that meristic data provide limited performance in morphometric analyses of mainland anoles. Nonetheless, these results should be interpreted with caution, as our study lacks morphometric information for almost 60% of the known species in the group.

Table 1. Comparison of meristic characters used in the taxonomy of the *latifrons* series sensu Poe et al. (2017) including the new species we described herein (see main text for details). Sources: 1– This study, 2 – Arosemena, Ibáñez & de Sousa, 1991, 3 – Ayala et al. (2021), 4 – Batista et al. (2015), 5 – Hulebak et al. (2007), 6 – Lotzkat et al. (2013), 7 – Poe and Ryan (2017), 8 – Poe et al. (2009), 9 – Rivero et al. (2009), 10 – Stejneger (1900), 11 – Velasco and Hurtado-Gómez (2014), 12 – Williams (1963), 13 – Williams (1975), 14 – Williams (1984), 15 – Williams (1984), 16 – Williams (1988) and 17 – Zambrano et al. (2024). Values in bold correspond to new data on the range of variation collected in this study; the remaining data were gathered from literature sources. The complete variable names are provided in the Morphological data section.

Species	Canths_2	PR	IO	IP/IO	SPLeye	PM	ToeLam2_3	ToeLam2_4	Source
<i>A. cyanophthalmus</i> sp. nov.	9–14	4–9	1–3	3–6	7–10	6–9	22–30	35–47	1
<i>A. agassizi</i>	–	–	–	–	–	–	36	–	10
<i>A. apollinaris</i>	8–16	8	2–4	2–5	7–8	5	23–29	41	1, 9, 16
<i>A. brooksi</i>	10–11	6–7	3–4	2–4	7–9	5–7	25–28	–	7
<i>A. casildae</i>	11–17	6–11	2–5	2–5	6–8	6–9	23	31–42	2, 6
<i>A. danieli</i>	8– 14	4–10	1–5	2–7	6–9	5–8	19–28	29–43	1, 16
<i>A. fraseri</i>	6–10	5–9	2–5	2–5	6–9	4–8	18–24	28	3, 16
<i>A. frenatus</i>	9–15	5–9	2–5	3–6	8–12	6–11	22–30	35–43	1, 2, 6, 16
<i>A. ginaelisae</i>	5–9	4–8	1–3	3	6–8	4–7	–	29–36	6
<i>A. ibanezi</i>	8–12	6–8	2–3	2–3	7–8	6–8	17–19	27–30	4, 6, 8
<i>A. insignis</i>	9–11	7–10	2–3	2–3	8–9	6–9	25–27	37–41	7
<i>A. kathydayae</i>	9–11	5–6	3–4	3–4	7–8	4–5	23–27	–	7
<i>A. kunayalae</i>	12–17	6–9	4–5	3–6	7–10	6–8	11–15	18–24	4, 5, 6
<i>A. latifrons</i>	11–15	6–9	3–5	4–8	8–11	6–10	21–27	36–43	1, 4, 16
<i>A. limon</i>	8– 12	5–9	1–3	1–5	8–10	6–8	19–25	28–36	1, 11, 17
<i>A. maculigula</i>	12–19	7–11	1–5	0–3	6–10	4–12	16–23	29–35	1, 15
<i>A. maia</i>	10–16	6–8	2–3	3–5	9–11	6–7	–	28–32	4
<i>A. microtus</i>	6–9	5–7	1–2	1	7–9	6–8	20–22	32–34	2, 6, 16
<i>A. mirus</i>	12– 14	6–7	4–5	3–4	7–10	6–8	15–18	25–26	1, 12, 13
<i>A. nemontae</i>	7–11	6–9	3–4	2–3	7–10	5–7	21–23	–	3
<i>A. parilis</i>	17	6	4	6	9	8	15	–	13
<i>A. princeps</i>	12–17	5–9	2–6	3–7	9–12	6–11	22–25	39–40	1, 16
<i>A. purpurescens</i>	7– 15	5–10	1–5	2–6	7–10	1–7	18–21	25–33	1, 4
<i>A. propinquus</i>	12	6	3	–	7–8	6	25	–	14, 16
<i>A. savagei</i>	8–9	6–7	2	1–2	7	7–8	25–29	–	7
<i>A. squamulatus</i>	11–15	–	3–5	4–8	6–11	–	22–27	–	16

Biogeography

Our reconstructed phylogeny places the highland species *Anolis danieli* as sister to the remaining green anoles distributed in the mid-elevation areas of the Magdalena Valley (*A. limon*), the Pacific lowlands of Colombia (*A. purpurescens*), and the lowlands of Panama (*A. ibanezi* and *A. maia*). This branching pattern suggests that diversification within the clade occurred along a highland-lowland axis, potentially involving an ancestor inhabiting the highlands of the Western Cordillera. Subsequent downslope range expansion and dispersal toward the western slope of the Central Cordillera, and ultimately into the Pacific region and Panama, may have driven a rapid radiation of the mid- to lowland subclade. A highland origin followed by downslope diversification has also been hypothesized for other anoles and frogs from montane regions of South America (Firkowski et al. 2016; Prates et al. 2020). Moreover, this scenario may help explain the close phylo-

genetic relationships, low genetic distances, and morphometric overlap observed among species in this subclade.

The species previously misidentified as *Anolis danieli* and its sister species (*A. sp.2* sensu Castañeda and de Queiroz 2011) are allopatrically distributed, with the former occurring on the eastern slope of the Central Cordillera between 1500 and 1900 m a.s.l. and the latter on the western slope of the Eastern Cordillera at 1360 m a.s.l. approximately (Castañeda and de Queiroz 2011). During the late Miocene, when the divergence of both species is estimated to have occurred (Prates et al. 2017, 2020), the Eastern Cordillera underwent a dynamic uplift phase, reaching elevations between 1600 and 2100 m a.s.l. (Boschman 2021). Such intensive orogenic activity may have influenced the divergence of these species by splitting the range of a putative ancestral population, a mechanism also implicated in the diversification of the highland Andean anoles of the *heterodermus* series (Moreno-Arias et al. 2023).

Taxonomic comments in the *latifrons* series

It is worth noting that although we used the same sequences reported in Poe et al. (2015) and Poe and Ryan (2017) for *A. insignis*, *A. brooksi*, and *A. kathydayae*, a direct comparison with those studies is limited, as they presented cladograms rather than phylograms, thereby omitting branch length information. Our phylogenetic reconstruction supports *A. insignis* as a distinct lineage. However, both our phylogram and genetic distance analysis revealed insufficient genetic divergence to support *A. brooksi* and *A. kathydayae* as separate species (Figs 1, 3). Poe and Ryan (2017) assigned a population from Panama, previously considered part of *A. insignis*, to the species *A. brooksi*, which they redescribed. They also used a combined genetic and morphological analysis to describe *A. kathydayae*. However, they acknowledged that their genetic data provided limited support for the recognition of the newly described taxa and that their justification for these species relied primarily on morphological differences. However, we gathered information on the range of meristic values reported by the authors in their description of these species and found a high overlap among them (see Table 1). Thus, the low genetic distances, short branch lengths connecting *A. kathydayae* and *A. brooksi*, and the high overlap in meristic values suggest that these two nominal species represent a single taxon. Therefore, in accordance with the principle of priority, *A. kathydayae* should be considered a junior synonym of *A. brooksi*. Additional genetic data are required to determine whether the population from Darién (Panama), previously considered part of the range of *A. insignis* and described under the name *A. savagei*, is actually conspecific with *A. brooksi* or instead represents a distinct evolutionary lineage.

Reconstructing the molecular phylogeny of the *latifrons* series entailed several challenges related to the accuracy of information linked to sequence vouchers. For example, some sequences have been deposited in GenBank under inconsistent or ambiguous voucher codes, (e.g., field and museum codes) and even the names of some vouchers differ across studies, thus complicating efforts to confidently associate them with specific taxa. Additionally, several vouchers retain outdated species names. For example, the vouchers SL 646 (SMF 91477) and SL 131 (SMF 89482) are labeled as *A. insignis* in GenBank despite these specimens having been named *A. kathydayae* and *A. brooksi* by Poe and Ryan (2017).

These issues are further exacerbated by the frequent absence of geographic coordinates tied to vouchers, complicating efforts to assess the geographic distribution limits among lineages. This limitation is particularly pronounced in species described early in the systematic history of the group, for which locality data are often imprecise, vague, or entirely missing. In some instances, even the holotype specimen or its associated data are currently lost (e.g., *Anolis insignis* and *A. frenatus*), further complicating efforts to reconcile historical taxonomy with contemporary phylogenetic frameworks. Based on these observations, we strongly encourage researchers to deposit sequence data

in public repositories, accompanied by complete metadata, including accurate geographic coordinates. Making raw datasets (e.g., morphological measurements) openly available is also essential for enabling their inclusion in complementary studies. By adopting these practices, we will enhance research transparency, support robust hypothesis testing, and facilitate the reproducibility of studies. Following these principles, we are releasing in public repositories not only the newly generated sequences but also the voucher information with geographic coordinates and the raw data of morphological variables.

Lastly, we acknowledge that our phylogeny, although representing the most comprehensive hypothesis for the *latifrons* series to date, remains incomplete, as it does not include the species *Anolis propinquus*, *A. squamulatus*, and *A. savagei*. These species were included in the phylogenies of Poe et al. (2017) and Poe and Ryan (2017); however, as with *A. limon* and *A. mirus*, their placement was based solely on morphological data. Therefore, formal testing of the phylogenetic positions of these three species within a molecular framework is needed, given that, as we have shown, incorporating DNA sequences for species previously evaluated only through morphology as well as increasing taxon sampling led to rearrangements in the inferred evolutionary relationships within the *latifrons* series.

Our phylogenetic reconstruction, together with genetic and morphological data, consistently supports the conclusion that the lineage identified as *Anolis danieli* in the phylogeny of Castañeda and de Queiroz (2011) and subsequent studies represents an undescribed taxon, which we describe below.

Taxonomy

Anolis cyanophthalmus sp. nov.

<https://zoobank.org/8E0FC7AB-C20E-4D0B-9D5F-1D8B68D9FFB8>

Figures 5–7A–C; Table 1

Chresonymy.

Anolis danieli Anorí, *Anolis danieli* “anorí” – Velasco and Hoyos (2010), pp. 206, 207, figs 1, 3B

Anolis danieli – Castañeda and de Queiroz (2011), p. 797, table 1 [MHUA 11564, MHUA 11567]

Anolis danieli – Batista et al. (2015), p. 71, fig. 7 [MHUA 11564, MHUA 11567]

Anolis danieli – Poe et al. (2017), p. 668, fig. 1

Anolis danieli – Prates et al. (2017), p. 52, fig. 2 [MHUA 11564]

Anolis danieli – Torres-Carvajal et al. (2017), p. 3, table 1 [MHUA 11564, MHUA 11567]

Anolis danieli – Prates et al. (2020), p. 6, fig. 3 [MHUA 11564]

Anolis danieli – Ayala-Varela et al. (2021), p. 310, fig. 9 [MHUA 11564, MHUA 11567]

Holotype (Fig. 6). COLOMBIA • 1 ♂, adult, with hemipenis in a separate vial; Department of Antioquia, municipality of Yarumal, Vereda El Rosario, Natural Reserve El Reposo; 7.062, –75.404; 1570 m a.s.l.; 30 Sep. 2018; Mauricio Rivera-Correa leg.; MHUA-R 13757.

Paratypes. COLOMBIA • 1 ♂, juvenile; Department of Antioquia, municipality of San Rafael, Vereda Cirpes, Central Hidroeléctrica Peñol-Guatapé; 6.277, –75.144; 1830 m a.s.l.; 14 Oct. 2023; Carlos M. Marín & Daniel Bocanumenth leg.; MHUA-R 15831. • 1 juvenile; same locality as for preceding; 6.2750, –75.1453; 1905 m a.s.l.; 17 Oct. 2023; Carlos M. Marín & Daniel Bocanumenth leg.; MHUA-R 15833. • 2 ♀, adult; Department of Antioquia, municipality of Anorí, Vereda El Roble, Finca El Chaquiral; 6.981, –75.136; 1725 m a.s.l.; 2003; Paul D. Gutiérrez leg.; MHUA-R 11008, MHUA-R 11289. • 1 ♂, adult, with hemipenis in a separate vial; Department of Antioquia, municipality of Anorí, Vereda Cañada Honda, Quebrada La Soledad; 7.005, –75.146; 1640 m a.s.l.; 7 Jan. 2004; Paul D. Gutiérrez leg.; MHUA-R 11293. • 1 ♀, adult; same locality as for preceding; MHUA-R 11302. • 1 ♀, juvenile; Department of Antioquia, municipality of Anorí, Vereda Cañada Honda; 7.005, –75.146; 1666 m a.s.l.; 2–5 Jan. 2007; Paul D. Gutiérrez leg.; MHUA-R 11564. • 4 ♀, adults; same locality as for preceding; MHUA-R 11565, MHUA-R 11567, MHUA-R 1570 to 1571. • 2 ♀, adults; Department of Antioquia, municipality of Anorí, Vereda El Nevado; 6.992, –75.119; 1650 m a.s.l.; 6 Jan. 2007; Laura Bravo leg.; MHUA-R 11594 to 11595. • 1 ♂, juvenile; Department of Antioquia, municipality of Anorí, Vereda El Retiro, Finca El Chaquiral; 6.979, –75.129; 1768 m a.s.l.; 13 Jun. 2015; JMD leg.; MHUA-R 12834. • 1 ♂, juvenile; Department of Antioquia, municipality of Yarumal, Vereda El Rosario, Natural Reserve El Reposo; 7.062, –75.404; 1570 m a.s.l.; 30 Sep. 2018; Mauricio Rivera-Correa leg.; MHUA-R 13756.

Diagnosis. We assign *Anolis cyanophthalmus* **sp. nov.** to the *Dactyloa* clade within *Anolis* based on our phylogenetic results. *Anolis cyanophthalmus* **sp. nov.** differs from species in the *punctatus* and *heterodermis* series (Castañeda and de Queiroz 2011) by having smaller head scales; from species in the *nasofrontalis* and *roquet* series (Poe et al. 2017; Prates et al. 2020) by having supraorbital semicircles separated from each other and the interparietal separated from the supraorbital semicircles; and from species in the *aequatorialis* series (Castañeda and de Queiroz 2011; Prates et al. 2020) by having wider toepads and larger dorsal head scales.

Description of holotype (paratypes variation in parentheses). Frontal depression present; head dorsal scales small, rugose to keeled in the nasal and frontal region; rugose to keeled internasals; deep parietal depression; parietal region with juxtaposed, mostly hexagonal scales; postrostrals six (5–9); supraorbitals larger than adjacent scales, polygonal, smooth to rugose (smooth to keeled), and separated by two (0–2) scales from supraorbital semi-

circles; some enlarged and keeled scales in the supraocular disc, the remaining smooth; scales between interparietal and supraorbital semicircles heterogeneous in size; interparietal longer than wide, slightly rectangular, much larger than adjacent scales, smaller than ear opening, and separated by four small scales from supraorbital semicircles (3–6); parietal scales slightly rugose; canthals keeled; circumnasal rounded; prenasal single contacting two rostral scales (lower prenasal in MHUA-R: 11293, 11302, 11564, 11567, 11570, 11594, 12834, 15833); canthal scales ten (8–11); anterior canthals contacting circumnasals; scales between second canthals twelve (9–14); loreal rows eight (6–8), keeled, upper contacting the first and second canthals; three suboculars in broad contact with the supralabials, no scales rows between suboculars and supralabials; temporals small and granular; supralabials to the center of the eye eight (8–10); ear opening oval-shaped, surrounded by small granular scales; anterior edge of rostral ventrally visible; mental semicircular, concave and divided; infralabials in eight rows; sublabial scales not enlarged; postmentals eight (6–9).

Trunk. Middorsal and paravertebral scales are small and keeled, and slightly larger than flanking scales, which are granular and separated by small skin interspaces; ventral scales smooth and imbricate, with rounded posterior margins and larger than dorsal scales; groin, axilla and neck covered by granular scales; nuchal and dorsal folds present in males, absent in females; two enlarged postanal scales in males, absent in females.

Limbs. Fore and hind limbs with keeled scales; hind limbs robust, 1.6 times longer than forelimbs; fourth toe lamellae under phalanges II–III 27 (22–30) and under phalanges II–IV 41 (35–47); cylindrical limbs, with keeled and imbricated scales; anterior part of the arm and elbow with uncarinate scales; thigh with uncarinate scales, knee with strongly keeled scales; ventral scales smooth, imbricate and with rounded posterior margins; tail with keeled scales and three middorsal rows (Fig. 6).

Dewlap. 37.74 mm in length and 21.10 mm in height (paratypes: adult males 41.01 ± 5.72 mm [36.13–50.07] in length, 23.85 ± 8.60 mm [14.44–37.87] in height, $n = 3$; adult females 20.67 ± 2.25 mm [18.08–23.65] in length, 10.36 ± 1.53 mm [7.92–11.85] in height, $n = 5$); dewlap extends posteriorly to arms in males and slightly beyond the insertion of the arms in females (Fig. 11); seven longitudinal scale rows (7–9), formed by 3–4 (2–5) pale cream scales and separated by pale cream naked skin in males, and five rows (4–6) formed by 2–4 pale scales and separated by dark brown naked skin in females.

Color in life (Fig. 5). Coloration in life is described based on information gathered from the paratypes MHUA-R 15831 and 15833, both males, the photographs of the holotype (Fig. 7A) and specimens from the iNaturalist platform. The head surface is greenish to pale brown with a transverse interorbital yellow band delineated by narrow dark brown lines; superciliary scales are solid yel-



Figure 5. Paratype of *Anolis cyanophthalmus* **sp. nov.** juvenile male MHUA-R 15831 in life. SVL 72.56 mm. Photo by Daniel Bocanumenth.

low; a post-ocular wide band extends to the upper level of the ear opening; a sub-ocular dark brown band extends posteriorly at the level of the postocular band, and a light cream band extends from the posteriormost supralabial scales upward to the loreal region; yellow supralabial scales becomes pale brown posteriorly; gray-bluish bands extending from the infralabials into the gular region; lateral dark green-yellowish blotches in the neck and the anterior region of the arm insertion; a dark brown band extends from the arm insertion to the upper level of the posteriormost supralabial scales; iris blue-grayish; tongue cream; in males, the naked skin of dewlap is pale gray-bluish with cream longitudinal scales rows; in females, the naked skin of the dewlap is dark brown with beige longitudinal scale rows; dorsum cream to greenish with dark brown transverse bands bordered by greenish brown, extending to the flanks and forming an inverted V-shaped pattern; greenish transverse bands in the dorsal surfaces of the arms and legs extending to the fingers and toes where they become narrow; light small dots along the transverse bands in the dorsum and legs but absent in the tail's bands; transverse dark bands on the first third of the tail's length, followed by a solid dark coloration in the second third, and a pale greenish solid coloration in the remaining third of the tail; belly and ventral surfaces of the arms and legs cream with small yellow blotches; throat yellowish with small gray-bluish blotches; yellowish mental and infralabial scales; yellowish postcloacal scales and ventral surface of the tail cream yellowish.

Color in preservative (Fig. 6). Head surface pale brown without evident patterns; dorsum pale to dark cream with transverse dark brown bands extending to the flanks and

forming an inverted V-shaped pattern, which further extends to the middle region of the tail and the dorsal surfaces of arms and legs (in older specimens, coloration becomes darker). White small dots in the lateral transverse bands on the trunk. The belly is uniformly pale cream, (in older specimens it turns into a pale brown color). The second half of the ventral surface of the tail is dark brown. In males, the naked skin of the dewlap is gray bluish with longitudinal rows of pale brown scales; in females, the naked skin of the dewlaps is dark brown with longitudinal rows of cream scales. The dorsal surface of arms and legs is pale cream without evident marks or patterns, turning into pale brown in older specimens (Fig. 6).

Comparisons with other species. As *Anolis cyanophthalmus* **sp. nov.** belongs to the *latifrons* series, we compared it with the remaining species within this clade. Comparisons were conducted by a detailed revision of the original descriptions and, when possible, by direct examination of museum specimens. Comparing the remaining species of the *latifrons* series, *Anolis cyanophthalmus* **sp. nov.** differs from *A. ginaelisae* (Lotzkat, Hertz, Bienenreut & Köhler, 2013) and *A. microtus* Cope, 1871 by having higher number of scales between the second canthals (9–14 in *A. cyanophthalmus* **sp. nov.** vs 5–9 in *A. ginaelisae* and 6–9 in *microtus*); from *A. parilis* by having fewer scales between the second canthals (9–14 in *A. cyanophthalmus* **sp. nov.** vs 17 in *A. parilis*); from *A. kunayalae*, *A. mirus* and *A. latifrons* by having fewer scales between supraorbital semicircles (1–3 in *A. cyanophthalmus* **sp. nov.** vs 4–5 in both *A. kunayalae* and *A. mirus* and 3–5 in *A. latifrons*); from *A. maculigula* and *A. savagei* by having higher number of scales

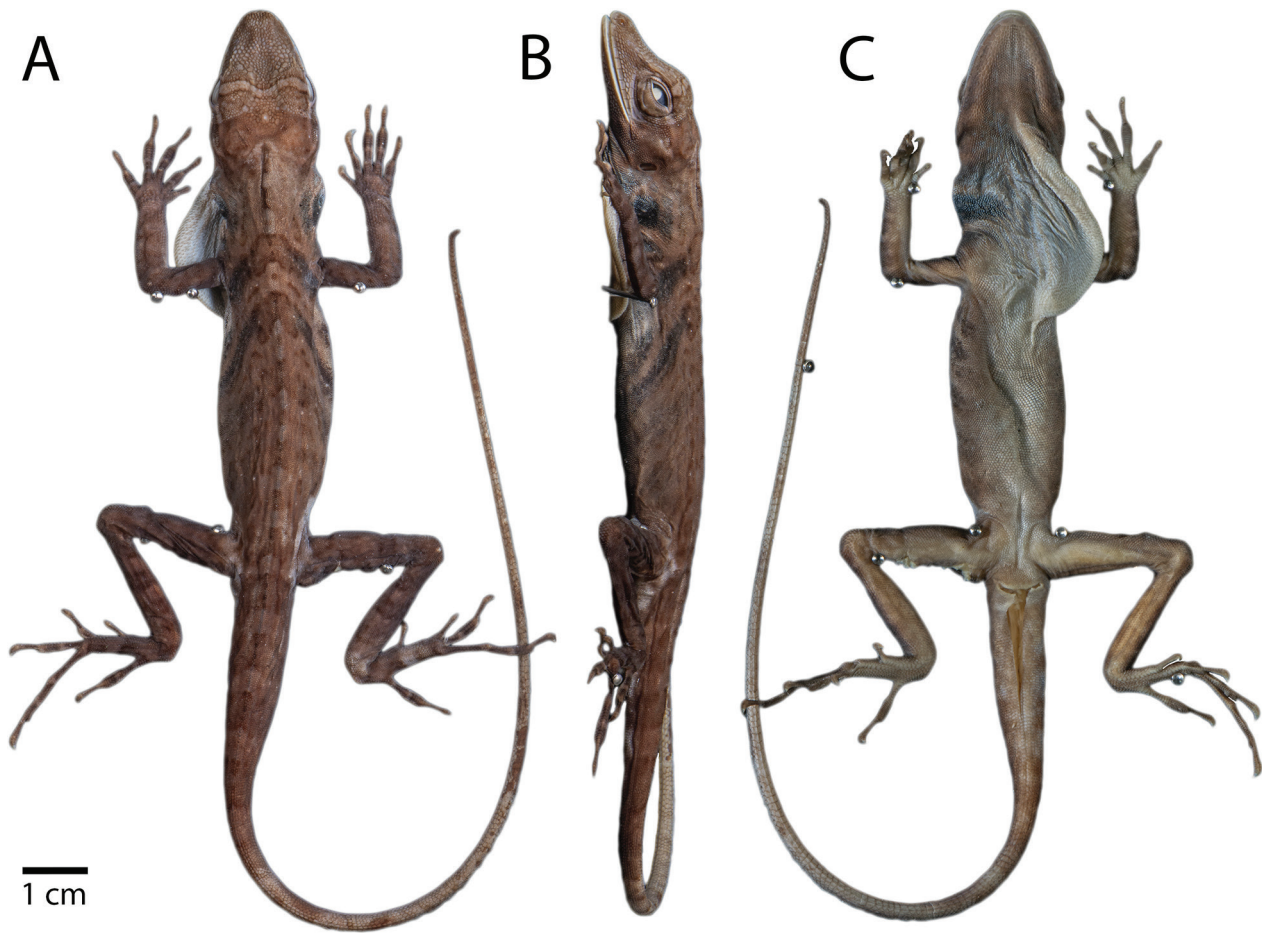


Figure 6. Holotype of *Anolis cyanophthalmus* sp. nov. (MHUA-R 13757 adult male). **A** dorsal, **B** lateral, **C** ventral views. SVL = 86.55 mm. Photos by Daniel Bocanumenth.

between interparietal and semicircles (3–6 in *A. cyanophthalmus* sp. nov. vs 1–3 in *A. maculigula* and 1–2 in *A. savagei*); from *A. purpurescens* and *A. propinquus* by having high number of postmentals (6–9 in *A. cyanophthalmus* sp. nov. vs 1–7 in *A. purpurescens* and 6 in *A. propinquus*); from *A. agassizi* Stejneger, 1900 by having lower number of lamellae under the phalanges II–III of fourth toe (22–30 in *A. cyanophthalmus* sp. nov. vs 36 in *A. agassizi*); from *A. ibanezi*, *A. limon*, and *A. maia* by having higher number of lamellae under the phalanges II–III of fourth toe (22–30 in *A. cyanophthalmus* sp. nov. vs 17–19 in *A. ibanezi*, 20–22 in *A. limon* and 19–21 in *A. maia*); and from both *A. danieli* and *A. frenatus* by having smaller body size (mean SVL = 87.2 ± 12.6 mm [males], 69.3 ± 12.4 mm [females] in *A. cyanophthalmus* sp. nov. vs 107.9 ± 10.1 [males], 93.7 ± 7.4 mm [females] in *A. danieli* and 129.3 ± 2.5 mm [males], 100 ± 8.4 mm [females] in *A. frenatus*). A summary of the meristic traits used in the above comparisons is shown in Table 1. A comparison of color patterns among the species analyzed in this study is shown in Figure 7.

A species that can potentially be confused with *Anolis cyanophthalmus* sp. nov. is *A. anoriensis* Velasco, Gutiérrez-Cárdenas & Quintero-Angel, 2010. This latter species occurs in the northern region of the Central Cordillera, in the municipalities of Anori and Guatapé (Marín et al. 2017), making it sympatric with the new species across

a large part of its distribution range. However, *A. cyanophthalmus* sp. nov. differs from *A. anoriensis* in the male dewlap coloration pattern (background pale cream with eight scales rows in *A. cyanophthalmus* sp. nov. vs. background with both yellowish and brown blotches with 5 rows of yellow scales in *A. anoriensis*) and in having fewer scales between the second canthals (8–11 in *A. cyanophthalmus* sp. nov. vs. 11–15 in *A. anoriensis*).

Etymology. The specific epithet *cyanophthalmus* is derived from the Greek *kyanos* (blue) and *ophthalmos* (eye) and is used as a latinized adjective referring to the remarkable iris coloration of the new species, which ranges from blue to blue-green hues.

Suggested Common Name. Colombian blue-eyed anole [English]. *Anolis* de ojos azules [Spanish]

Distribution and natural history. *Anolis cyanophthalmus* sp. nov. inhabits the premontane forests of the northern Central Cordillera in the department of Antioquia, Colombia, at elevations between approximately 1500 and 2000 m a.s.l. (Fig. 1). Additionally, there is a photographic record on the iNaturalist platform (<https://www.inaturalist.org/observations/5625949>) from the eastern versant of the Central Cordillera in the department of Tolima, Colombia, at 1200 m a.s.l., representing a specimen that

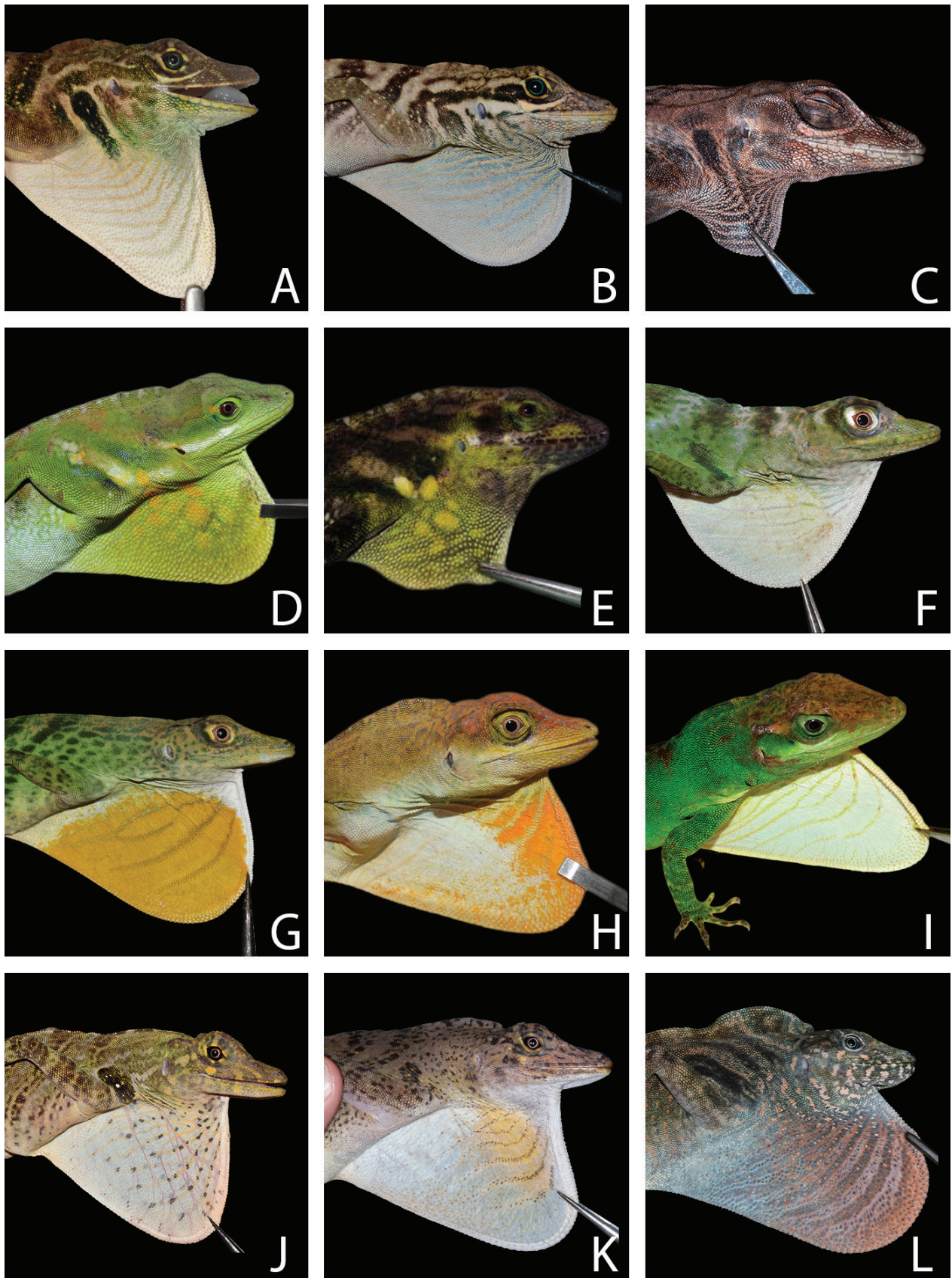


Figure 7. Dewlap coloration of *Anolis cyanophthalmus* sp. nov. and related spp. **A** *A. cyanophthalmus* sp. nov. (MHUA-R 13757, holotype, photo by M. Rivera-Correa), **B** *A. cyanophthalmus* sp. nov. (MHUA-R 15831, paratype, photo by D. Bocanumenth), **C** *A. cyanophthalmus* sp. nov. (MHUA-R 11302, paratype in preservative, photo by D. Bocanumenth), **D** *A. danieli* (MHUA-R 13061, photo by F. Grisales-Martínez), **E** *A. danieli* (CSJ-H 5025, photo by L.M. Solano), **F** *A. limon* (MHUA-R 13476, photo C.M. Marín), **G** *A. purpurescens* (MHUA-R 15867, photo by C.M. Marín), **H** *A. fraseri* (MHUA-R 13846, photo by F. Grisales-Martínez), **I** *A. mirus* (MHUA-R 12625, photo by E. Alzate Basto), **J** *A. latifrons* (MHUA-R 15881), **K** *A. frenatus* (MHUA-R 12906) and **L** *A. maculigula* (MHUA-R 12965). All individuals are adults (except D) and males (except C and E).

we assign to this species. Only two specimens are known from the municipality of Yarumal, collected in 2018, and two additional specimens were recorded during recent fieldwork in the municipality of San Rafael. These two individuals were found perched on bush branches at a height of approximately 1.5 meters. The small number of specimens observed in the Yarumal and San Rafael municipalities suggests that local populations of this species occur at low densities, as previously reported for the population in Anorí (Molina-Zuluaga and Gutiérrez-Cárdenas 2007). The population of *Anolis cyanophthalmus* **sp. nov.** from the municipality of San Rafael occurs within the protected areas surrounding the Peñol-Guatapé reservoir in the department of Antioquia, which may contribute positively to the future conservation status of the species.

Acknowledgments

CMM acknowledges the doctoral program of the Instituto de Ecología, A.C. (INECOL), Mexico, and the Secretaría de Ciencia, Humanidades, Tecnología e Innovación (SECIHTI) for support provided through the doctoral scholarship (2033788). We thank Esteban Garzón Franco and Andrea Bustamante Cadavid from the Museo de Ciencias Naturales de La Salle (CSJ), Carolina Torres Flórez from the Museo de Herpetología Universidad de Antioquia (MHUA), Juan Camilo Arredondo and Juan Manuel Lozano from Colecciones Biológicas de la Universidad CES (CBUCES), and Yehimy Xilena Rueda Isaza from Colección Biológica Universidad EAFIT for allowing us access to the specimens under their care. We thank A. Katerine Rodríguez for helping us with the vocabulary of morphometric variables. We thank Yeison Tolosa, Mauricio Rivera-Correa, Freddy A. Grisales-Martínez, Luis Manuel Solano Redondo, and Esteban Alzate Basto for allowing us to use their photographs and observations.

References

- AYALA-VARELA F, VALVERDE S, POE S, NARVÁEZ AE, YÁNEZ-MUÑOZ MH, TORRES-CARVAJAL O (2021) A new giant anole (Squamata: Iguanidae: Dactyloinae) from southwestern Ecuador. *Zootaxa* 4991: 295–317. <https://doi.org/10.11646/zootaxa.4991.2.4>
- AYALA-VARELA FP, VELASCO JA (2010) A new species of dactyloid anole (Squamata: Iguanidae) from the western Andes of Ecuador. *Zootaxa* 2577: 46–56. <https://doi.org/10.11646/zootaxa.2577.1.2>
- BATISTA A, VESELY M, MEBERT K, LOTZKAT S, KÖHLER, G (2015) A new species of *Dactyloa* from eastern Panama, with comments on other *Dactyloa* species present in the region. *Zootaxa* 4039: 57–84. <https://doi.org/10.11646/zootaxa.4039.1.2>
- BOSCHMAN LM (2021) Andean mountain building since the Late Cretaceous: A paleoelevation reconstruction. *Earth-Science Reviews* 220: 103640. <https://doi.org/10.1016/j.earscirev.2021.103640>
- CASTAÑEDA M, DE QUEIROZ K (2011) Phylogenetic relationships of the *Dactyloa* clade of *Anolis* lizards based on nuclear and mitochondrial DNA sequence data. *Molecular Phylogenetics and Evolution* 61: 784–800. <https://doi.org/10.1016/j.ympev.2011.07.004>
- CASTAÑEDA M, DE QUEIROZ K (2013) Phylogeny of the *Dactyloa* clade of *Anolis* lizards: New insights from combining morphological and molecular data. *Bulletin of the Museum of Comparative Zoology* 160: 345–398. <https://doi.org/10.3099/0027-4100-160.7.345>
- CHRISTODOULIDES N, URGILES VL, GUAYASAMÍN JM, SAVAGE AE (2024) Selection and gene duplication associated with high-elevation diversification in *Pristimantis*, the largest terrestrial vertebrate genus. *Genome Biology and Evolution* 16: evae167. <https://doi.org/10.1093/gbe/evae167>
- ETHERIDGE R (1960) The relationships of the anoles (Reptilia: Sauria: Iguanidae): An interpretation based on skeletal morphology. PhD Thesis, University of Michigan, Ann Arbor, MI, 236 pp.
- FIRKOWSKI CR, BORNSCHEIN MR, RIBEIRO LF, PIE MR (2016) Species delimitation, phylogeny and evolutionary demography of co-distributed, montane frogs in the southern Brazilian Atlantic Forest. *Molecular Phylogenetics and Evolution* 100: 345–360. <https://doi.org/10.1016/j.ympev.2016.04.023>
- GRISALES-MARTÍNEZ FA, VELASCO JA, BOLÍVAR W, WILLIAMS EE, DAZA JM (2017) The taxonomic and phylogenetic status of some poorly known *Anolis* species from the Andes of Colombia with the description of a nomen nudum taxon. *Zootaxa* 4303: 213–230. <https://doi.org/10.11646/zootaxa.4303.2.2>
- JOMBART T (2008) adegenet: A R package for the multivariate analysis of genetic markers. *Bioinformatics* 24: 1403–1405. <https://doi.org/10.1093/bioinformatics/btn129>
- JOMBART T, DEVILLARD S, BALLoux F (2010) Discriminant analysis of principal components: A new method for the analysis of genetically structured populations. *BMC Genetics* 11: 94. <https://doi.org/10.1186/1471-2156-11-94>
- KALYAANAMOORTHY S, MINH BQ, WONG TKF, VON HAESLER A, JERMIIN LS (2017) ModelFinder: Fast model selection for accurate phylogenetic estimates. *Nature Methods* 14: 587–589. <https://doi.org/10.1038/nmeth.4285>
- KATOH K, STANDLEY DM (2013) MAFFT multiple sequence alignment software version 7: Improvements in performance and usability. *Molecular Biology and Evolution* 30: 772–780. <https://doi.org/10.1093/molbev/mst010>
- KÖHLER G (2014) Characters of external morphology used in *Anolis* taxonomy – Definition of terms, advice on usage, and illustrated examples. *Zootaxa* 3774: 201–257. <https://doi.org/10.11646/zootaxa.3774.3.1>
- KÖHLER G, SUNYER J (2008) Two new species of anoles formerly referred to as *Anolis limifrons* (Squamata: Polychrotidae). *Herpetologica* 64: 92–108. <https://doi.org/10.1655/07-027.1>
- MARÍN CM, VÁSQUEZ-RESTREPO JD, SEPÚLVEDA JD, DAZA JM (2017) On geographic distribution and morphological variation of the poorly known lizard *Anolis anoriensis* Velasco, Gutiérrez-Cárdenas & Quintero-Angel. *Herpetology Notes* 10: 643–645.
- MINH BQ, NGUYEN MAT, VON HAESLER A (2013) Ultrafast approximation for phylogenetic bootstrap. *Molecular Biology and Evolution* 30: 1188–1195. <https://doi.org/10.1093/molbev/mst024>
- MINH BQ, SCHMIDT HA, CHERNOMOR O, SCHREMPF D, WOODHAMS MD, VON HAESLER A, LANFEAR R (2020) IQ-TREE 2: New models and efficient methods for phylogenetic inference in the genomic era. *Molecular Biology and Evolution* 37: 1530–1534. <https://doi.org/10.1093/molbev/msaa015>
- MOLINA ZULUAGA C, GUTIÉRREZ CÁRDENAS DA (2007) Uso nocturno de perchas en dos especies de *Anolis* (Squamata: Polychrotidae) en un bosque Andino de Colombia. *Papéis Avulsos de Zoologia* 47: 273–281. <https://doi.org/10.1590/s0031-10492007002200001>
- MORENO-ARIAS RA, MÉNDEZ-GALEANO MA, BELTRÁN I, VARGAS-RAMÍREZ M (2023) Revealing anole diversity in the highlands of the Northern Andes: New and resurrected species of the *Anolis heterodermus* species group. *Vertebrate Zoology* 73: 161–188. <https://doi.org/10.3897/vz.73.e94265>

- Palumbi SR (1996) Nucleic acids II: The polymerase chain reaction. In: Hillis DM, Moritz C, Mable BK (Eds) *Molecular Systematics*, Second Edition. Sinauer Associates, Sunderland, MA, 205–221.
- Paradis E, Claude J, Strimmer K (2004) APE: Analyses of phylogenetics and evolution in R language. *Bioinformatics* 20: 289–290. <https://doi.org/10.1093/bioinformatics/btg412>
- Poe S (2004) Phylogeny of anoles. *Herpetological Monographs* 18: 37–89. [https://doi.org/10.1655/0733-1347\(2004\)018\[0037:POA\]2.0.CO;2](https://doi.org/10.1655/0733-1347(2004)018[0037:POA]2.0.CO;2)
- Poe S, Latella I, Ayala-Varela F, Yañez-Miranda C, Torres-Carvajal O (2015) A new species of phenacosaur *Anolis* (Squamata; Iguanidae) from Peru and a comprehensive phylogeny of *Dactyloa*-clade anolis based on new DNA sequences and morphology. *Ichthyology & Herpetology* 103: 639. <https://doi.org/10.1643/CH-14-127>
- Poe S, Nieto-Montes de Oca A, Torres-Carvajal O, de Queiroz K, Velasco JA, Truett B, Gray LN, Ryan MJ, Köhler G, Ayala-Varela F, Latella I (2017) A phylogenetic, biogeographic, and taxonomic study of all extant species of *Anolis* (Squamata; Iguanidae). *Systematic Biology* 66: 663–697. <https://doi.org/10.1093/sysbio/syx029>
- Poe S, Ryan MJ (2017) Description of two new species similar to *Anolis insignis* (Squamata: Iguanidae) and resurrection of *Anolis (Diaphoranolis) brooksi*. *Amphibian & Reptile Conservation* 11: 1–16.
- Ponce M, Köhler G (2008) Morphological variation in anoles related to *Anolis kemptoni* in Panama. *Salamandra* 44: 65–83.
- Prates I, Melo-Sampaio PR, Drummond L de O, Teixeira M, Rodrigues MT, Carnaval AC (2017) Biogeographic links between southern Atlantic Forest and western South America: Rediscovery, re-description, and phylogenetic relationships of two rare montane anole lizards from Brazil. *Molecular Phylogenetics and Evolution* 113: 49–58. <https://doi.org/10.1016/j.ympev.2017.05.009>
- Prates I, Melo-Sampaio PR, Queiroz K De, Carnaval AC, Rodrigues MT, Drummond LDO (2020) Discovery of a new species of *Anolis* lizards from Brazil and its implications for the historical biogeography of montane Atlantic Forest endemics. *Amphibia Reptilia* 41: 87–103. <https://doi.org/10.1163/15685381-20191179>
- R Core Team (2025) R: A language and environment for statistical computing. R Foundation for Statistical Computing, Vienna. <https://www.R-project.org>
- Rivero EI, Veloza P, Rojas-Runjaic F (2009) Primer registro del lagarto *Anolis apollinaris*, para Venezuela. *Boletín del Centro de Investigaciones Biológicas* 43: 299–304.
- Santos JC, Coloma LA, Cannatella DC (2003) Multiple, recurring origins of aposematism and diet specialization in poison frogs. *Proceedings of the National Academy of Sciences of the USA* 100: 12792–12797. <https://doi.org/10.1073/pnas.2133521100>
- Santos JC, Coloma LA, Summers K, Caldwell JP, Ree R, Cannatella DC (2009) Amazonian amphibian diversity is primarily derived from Late Miocene Andean lineages. *PLoS Biology* 7: e1000056. <https://doi.org/10.1371/journal.pbio.1000056>
- Savage JM, Guyer C (1989) Infrageneric classification and species composition of the anole genera, *Anolis*, *Ctenonotus*, *Dactyloa*, *Norops* and *Semiurus* (Sauria: Iguanidae). *Amphibia-Reptilia* 10: 105–116.
- Savage JM, Talbot JJ (1978) The giant anoline lizards of Costa Rica and western Panama. *Copeia* 1978: 480–492. <https://doi.org/10.2307/1443615>
- Torres-Carvajal O, Ayala-Varela FP, Lobos SE, Poe S, Narváez AE (2018) Two new Andean species of *Anolis* lizard (Iguanidae: Dactyloinae) from southern Ecuador. *Journal of Natural History* 52: 1067–1089. <https://doi.org/10.1080/00222933.2017.1391343>
- Uetz P, Freed P, Aguilar R, Reyes F, Hošek J (Eds) (2023) The Reptile Database. <http://www.reptile-database.org> [accessed 5 Jun 2025].
- Velasco JA, Hoyos JM (2010) Phylogenetic analysis of the *latifrons* series of *Anolis* (Sauria: Iguania) with morphological data. *Anolis Newsletter* VI: 203–212.
- Velasco JA, Hurtado-Gómez JP (2014) A new green anole lizard of the *Dactyloa* clade (Squamata: Dactyloidae) from the Magdalena River valley of Colombia. *Zootaxa* 3785: 201–216. <https://doi.org/10.11646/zootaxa.3785.2.4>
- Velasco JA, Villalobos F, Diniz-Filho JAF, Poe S, Flores-Villela O (2020) Macroecology and macroevolution of body size in *Anolis* lizards. *Ecography* 43: 812–822. <https://doi.org/10.1111/ecog.04583>
- Williams EE (1975) South American *Anolis*: *Anolis parilis*, new species, near *A. mirus*. *Breviora* 434: 1–8.
- Williams EE (1976) South American anoles: The species groups. *Papéis Avulsos de Zoologia* 29: 259–268.
- Williams EE (1988) New or problematic *Anolis* from Colombia. V. *Anolis danieli*, a new species of the *latifrons* species group and a reassessment of *Anolis apollinaris* Boulenger, 1919. *Breviora* 489: 1–25.
- Williams EE, Rand H, Rand S, O'Hara R (1995) A computer approach to the comparison and identification of species in difficult taxonomic groups. *Breviora* 502: 1–47.
- Yáñez-Muñoz MH, Reyes-Puig C, Reyes-Puig JP, Velasco JA, Ayala-Varela F, TorresCarvajal O (2018) A new cryptic species of *Anolis* lizard from northwestern South America (Iguanidae, Dactyloinae). *ZooKeys* 2018: 135–163. <https://doi.org/10.3897/zookeys.794.26936>
- Zambrano DF, Gutierrez W, Zuñiga-Baos J, Cano K, Parra RM, Bernal MH (2024) New distribution records, morphology and natural history notes of the endemic Colombian lizard *Anolis limon*. *Herpetological Bulletin* 169: 7–11. <https://doi.org/10.33256/hb169.711>

Supplementary Material 1

Files S1–S5

Authors: Marín CM, Bocanumenth D, Daza JM (2025)

Data type: .zip

Explanation notes: **File S1.** Specimen data including museum, geographic, ENA/GenBank accession numbers and morphometric data [.xlsx file]. — **File S2.** Complete phylogenetic tree in newick format including 235 terminals (outgroups) [.contree file]. — **File S3.** Assembled genetic dataset including five genomic regions [.phy file]. — **File S4.** Nexus file describing the genomic partitions used in the phylogenetic analysis [.nex file]. — **File S5.** Heat map of net uncorrected genetic distances between species of the *latifrons* series as estimated using sequences of the COI fragment [.pdf file].

Copyright notice: This dataset is made available under the Open Database License (<http://opendatacommons.org/licenses/odbl/1.0>). The Open Database License (ODbL) is a license agreement intended to allow users to freely share, modify, and use this dataset while maintaining this same freedom for others, provided that the original source and author(s) are credited.

Link: <https://doi.org/10.3897/vz.74.e162071.suppl1>